The Influence of Particle Size and Surface Coating of Calcium Carbonate on the Rheological Properties of Its Suspensions in Molten Polystyrene

YOSHIYUKI SUETSUGU and JAMES L. WHITE, *Polymer Engineering, University of Tennessee, Knoxville, Tennessee 37996*

Synopsis

The rheological properties of polystyrene melts filled with 30 vol % of $CaCO_3$ particles of varying particle size are described. The influence of surface coating the particles with stearic acid is considered. Generally, the compounds with the uncoated particles exhibit viscosities which increase at ever greater rates as the shear rates decrease. It appears that these compounds exhibit yield values. Elongational flow data also suggest the existence of yield values. Difficulties exist in measurement of normal stresses in compounds with sizeable yield values. The principal normal stress difference at fixed shear stress of the PS/$CaCO_3$ compounds is lower than that of the PS melt. The magnitude of viscosity increases and yield values increase with decreasing particle size. Coating of particles with stearic acid results in major viscosity reductions and decreases in apparent yield values. The surface coating is most effective with the smallest particles. It presumably reduces interaction between particles and the extent of aggregation.

INTRODUCTION

The flow of particle-filled molten polymers has become of increasing importance in the plastics industry in recent years. Fillers often increase performance of polymeric products. They also frequently lower cost. There have been numerous studies of the rheological properties of particle filled polymer melts during the past 30 years.[1-25] These investigations generally show that the presence of particles increases the viscosity of the melt phase. The extent of viscosity rise was generally found to increase with volume loading[1-25] and with decreasing particle size.[6-8,12] Zakharenko et al.[4] appear to have been the first to conclude, at least on the basis of an extensive experimental study, that highly compounded polymer melts with small particles exhibited yield values. They studied rubber-carbon black compounds. Similar conclusions were reached a few years later by Chapman and Lee[6] for talc–polypropylene compounds. Succeeding researchers found similar behavior for titanium dioxide,[14,21,23] calcium carbonate,[17,19,21,23] and calcium sulfate anhydride fibers.[23] Compounds with large particles such as glass spheres[10,23] and glass, aramid, and cellulose fibers[16,22,23] do not exhibit yield values. The existence of yield values seems associated with small particle size.

Most studies of the rheological behavior of particle-filled polymer melts involve shear flow alone. Only investigators from our laboratories have considered the elongational as well as shear flow behavior of compounds with yield values.[20,21] These studies have indicated yield values in extension as well as shear. Han and his co-workers[11,24] and investigators from our laboratories[14,20,21,23] have studied

Journal of Applied Polymer Science, Vol. 28, 1481–1501 (1983)
 CCC 0021-8995/83/041481-21$03.10

normal stresses in compounds with small particles. These are found to be decreased at fixed shear stress.

A striking effect described by various researchers beginning with Chapman and Lee[6] is the result that certain additives or surface treatments cause considerable reductions in viscosities of polymer–particle compounds. This behavior has been described for talc,[6] titanium dioxide,[14] and calcium carbonate[18,21,24] compounds. There has, however, been little comprehensive study. Only two papers[21,24] effectively discuss more than shear flow of such systems.

It is our purpose in this paper to describe an experimental program which considers the influence of particle size and surface coating on the rheological behavior of particle-filled compounds. We choose polystyrene as the matrix and calcium carbonate as the particulate. The choice of calcium carbonate is due to its ready availability in a wide range of particle sizes. A series of rheological experiments will be reported on including (i) steady shear flow viscosity, (ii) steady shear flow principal normal stress difference, (iii) transient shear viscosity at the initiation of flow, (iv) transient shear viscosity in flows consisting of a shear flow followed by a rest period and a second shear flow, and (v) uniaxial elongational flow.

EXPERIMENTAL

Materials

The polymer used in this study was a commercial polystyrene (Dow Styron® 678U). The primary filler used in this study were calcium carbonates of varying particle size supplied by Pfizer. These are summarized in Table I. They were supplied in both their original form and coated with stearic acid. Compounds of 0.30 volume fraction filler (at 180 °C) were prepared on a two-roll mill at 150°C. The mixing process required 45 min. The polystyrene sample received a similar mastication history.

Shear Flow Measurements

Shear stress and principal normal stress differences were measured on a Rheometrics Mechanical Spectrometer at 180°C. A cone plate mode with a 0.1-rad cone angle and 1.25 cm cone radius was used.

TABLE I
Characteristics of Calcium Carbonate Particles

Filler	Supplier	Density at 180°C (g/cm^3)	Manufacturing process	Grade	Average particle size (μm)	BET surface area (m^2/g)
Uncoated calcium-carbonate	Pfizer	2.7	Natural ground	Marble white 325	17	1.2
				Vicron 15-15	3	3.6
			Precipitated	Albaglos	0.5	6.0
				Multifex MM	0.07	20
Coated calcium-carbonate			Natural ground	Marble White 325	17	1.2
				Hi-Phlex 100	3	3.6
			Precipitated	Super-Phlex 200	0.5	6.0
				Ultra-Phlex	0.07	20

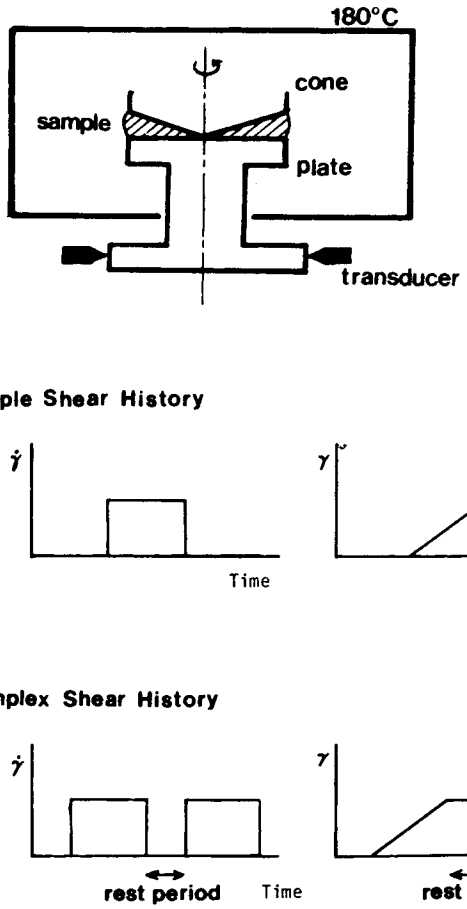

Fig. 1. Cone plate instrument with shear histories that samples are subjected to.

The milled samples were dried for 12 h in a vacuum oven and then compression molded into a 1.5-mm sheet preform for the mechanical spectrometer. These preforms were subsequently dried and placed in a dessicator. The preforms were pressed in several steps with intermediate trimmings into a 50-μm gap between the blunted tip of the cone and the plate. The samples were thermally equilibrated and allowed to relax for a period of 1 h before the beginning of the measurements. In the case of the compounds with the smaller uncoated particles the normal stresses do not fully relax.

The shear rate $\dot{\gamma}$ in the instrument was taken as[26,27]

$$\dot{\gamma} = \Omega/\alpha \tag{1}$$

where Ω is the angular velocity and α the cone angle.

The transient shear stress σ_{12} and the principal normal stress difference N_1 were determined from the expressions[26,27]

$$\sigma_{12} = 3M/2\pi R^3 \tag{2}$$

$$N_1 = 2F/\pi R^2 \tag{3}$$

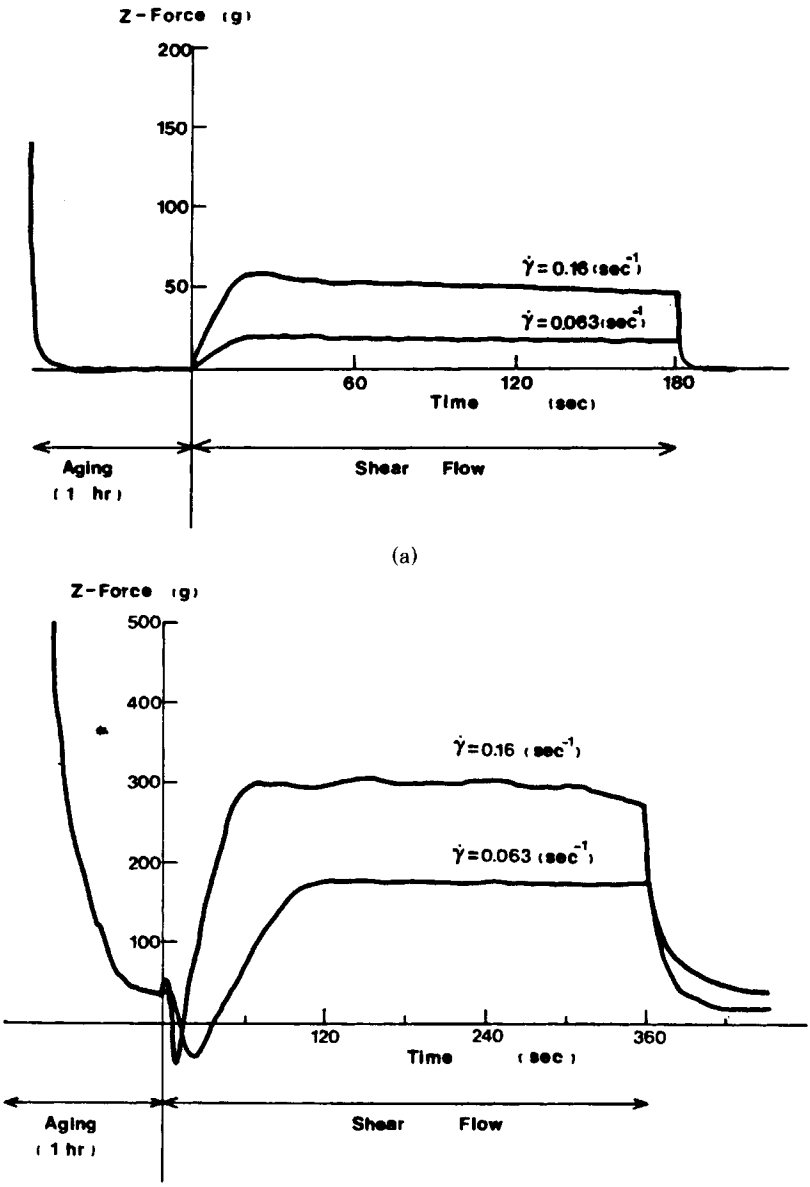

Fig. 2. Transient normal force–time traces for polystyrene: (a) polystyrene; (b) carbon-black-filled PS (ϕ = 0.3); (c) $CaCO_3$-filled PS (d_p = 0.5 μm) (ϕ = 0.3).

where M is the torque, R is the cone radius, and F the vertical Z force pushing apart the cone and plate.

Two types of shear histories were investigated in this study. In the first type, the sample was subjected to a steady shear history for a period of 15 min. The second history involves the sample being subjected to an initial steady shear rate deformation for 90 s, followed by a period of rest and a second constant shear rate history. The purpose of this second history was to investigate how long the

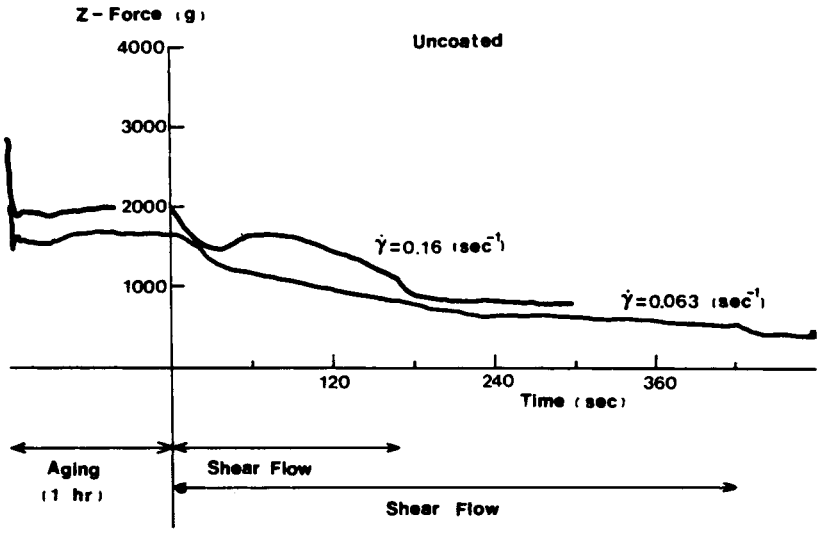

(c)

Fig. 2 (*Continued from the previous page.*)

compounds required to recover the characteristics of the virgin sample as compared to the pure polymer melt. These shear histories are shown in Fig. 1.

The possibility of slip of the compounds between the cone and plate was investigated by making fine straight lines on the sides of the sample and following their variation with time. No slip was observed.

The experiments were limited at high shear rates by instabilities on the outer edges of the sample. These have previously been observed for both homogeneous melts[28,29] and compounds.[19,20,23]

Some ambiguities arise with the normal force measurements. When the cone and plate are pressed together at the beginning of the experiment, the compressive force developed does not fully decay away [see Figs. 2(b), (c)]. The aging period on Figure 2 denotes the period between completing sample insertion and beginning of samples are shear deformation. Samples are sheared at $\dot{\gamma} = 0.063$ s^{-1} or 0.16 s^{-1} for the indicated periods. The vertical thrust F measured must involve some combination of this compressive force with the normal stresses developed in shear flow. Similar behavior has been observed with lubricating greases,[30,31] liquid crystalline cellulose derivatives,[32] and in our earlier studies of other compounds.[20,21]

Elongational Flow

Elongational flow measurements at a constant elongation rate in an instrument shown in Figure 3. This instrument is a modified version of an earlier apparatus developed in our laboratories by Ide and White,[33] but containing modifications suggested by the designs of Meissner.[34] The detailed design and development was carried out by Minoshima, Yamane, and the authors. The filaments were prepared by extrusion from a screw extruder at 180°C. The filament lies just

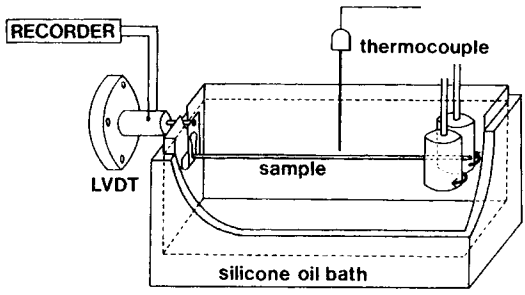

Fig. 3. Elongational flow rheometer.

below the surface of a silicone oil bath, and is clamped on one end to an LVDT and on the other to two gear wheels. This design leads to better temperature uniformity, defined filament length, and accuracy of measurement of tensile forces and stresses. The two gear rollers have a radius of 1.75 cm and are operated by two 1/15 HP B and B motors with a B and B controller. Elongation rates were achieved in the range of 4.66×10^{-3} to 1.47×10^{-1} s^{-1}. The deformation rate E and tensile stress σ_{11} were determined from

$$E = \frac{1}{L}\frac{dL}{dt} = \frac{R\Omega}{L} \tag{4}$$

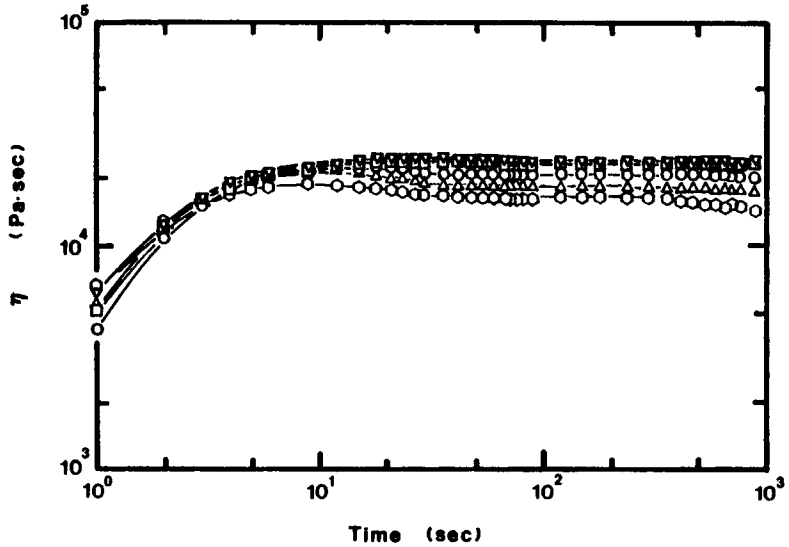

(a)

Fig. 4. Transient shear viscosities at the startup of flow $\dot{\gamma}$ (s^{-1}): (▽) 4.0×10^{-2}. (□) 6.3×10^{-2}; (○) 1.0×10^{-1}; (△) 1.6×10^{-1}; (○) 2.5×10^{-1}. (a) polystyrene; (b) polystyrene with 0.3 volume fraction $CaCO_3$ with particle diameter $d_p = 17$ μm; (c) polystyrene with 0.3 volume fraction $CaCO_3$ with particle diameter $d_p = 17$ μm; particles coated with stearic acid; (d) polystyrene with 0.3 volume fraction $CaCO_3$ with particle diameter $d_p = 3$ μm; (e) polystyrene with 0.3 volume fraction $CaCO_3$ with particle diameter $d_p = 3$ μm; particles coated with stearic acid.

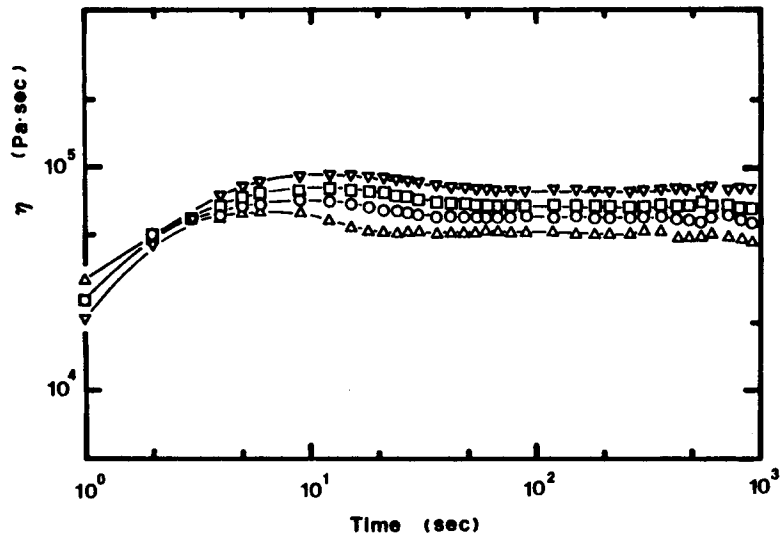

(b)

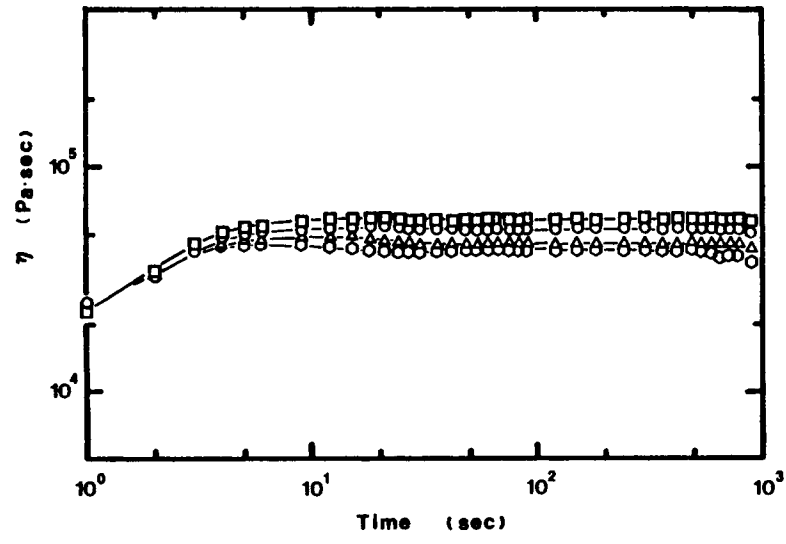

(c)

Fig. 4 (*Continued from the previous page.*)

$$\sigma_{11}(t) = \frac{F(t)}{A(t)} = \frac{F(t)}{A(0)} e^{Et} \tag{5}$$

where L is the filament length, Ω the rotation rate of the rolls, R the roll radius, F the tensile force, and A the cross-sectional area of the sample.

RESULTS

Shear Viscosity Transients

The variation of shear viscosity [i.e., $\sigma_{12}(t)/\dot{\gamma}$] at the initiation of flow in polystyrene (PS) and a series of CaCO-filled melts is shown in Figures 4(a)–(e).

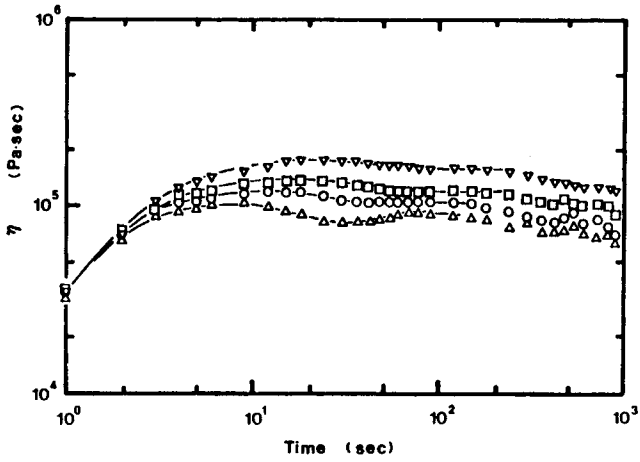

(d)

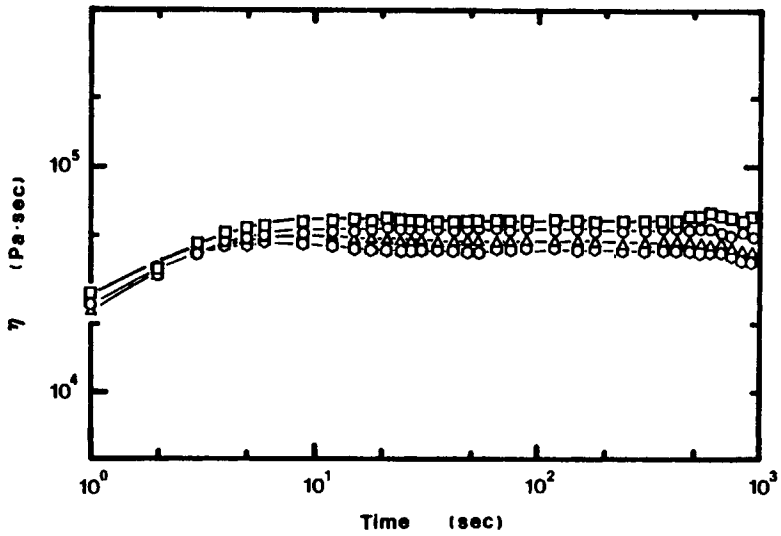

(e)

Fig. 4 (*Continued from the previous page.*)

The viscosities appear in the pure PS to slowly building up to a steady state at low $\dot{\gamma}$. At higher $\dot{\gamma}$, the viscosities overshoot and then decrease to the steady state. The viscosity overshoot tends to be greater for the compounds with small uncoated particles. We may quantify the stress overshoot through defining a function G:

$$G(\dot{\gamma}) = \frac{\sigma_{12}(\max, \dot{\gamma}) - \sigma_{12}(\infty, \dot{\gamma})}{\sigma_{12}(\infty, \dot{\gamma})} \tag{6}$$

We tabulate the $G(\dot{\gamma})$ function in Table II for two low shear rates. It may be seen that the largest $G(\dot{\gamma})$ are for the particle-filled melts. Surface coating reduces the stress overshoot.

TABLE II
Shear Stress Overshoot Function $G(\dot{\gamma})$ for Polystyrene and Particle Filled Melts

System	Particle diameter (μm)	Coating	$\dot{\gamma}$	$G(\dot{\gamma})$
PS	—	—	0.063	0.04
			0.16	0.13
$PS/CaCO_3$	17	no	0.063	0.18
	17	no	0.16	0.20
$PS/CaCO_3$	17	yes	0.063	0.01
	17	yes	0.16	0.09
$PS/CaCO_3$	3	no	0.063	0.13
	3	no	0.16	0.14
$PS/CaCO_3$	3	yes	0.063	0.01
	3	yes	0.16	0.09

Steady-State Viscosity

Steady state shear viscosities of PS and $PS/CaCO_3$ are shown as a function of shear rate in Figures 5 and 6 for the uncoated and coated particles. The viscosities of the compounds are all greater than the PS matrix. The viscosity increase is greatest for the uncoated particle compounds. From Figure 5, it may be seen that the viscosity increase is greatest for the compounds with the smallest particles.

The viscosity of the PS is constant at low shear rates and decreases with increasing shear rates. The compounds generally exhibit decreasing viscosities over the entire shear rate range. The rate of decrease of viscosity becomes even

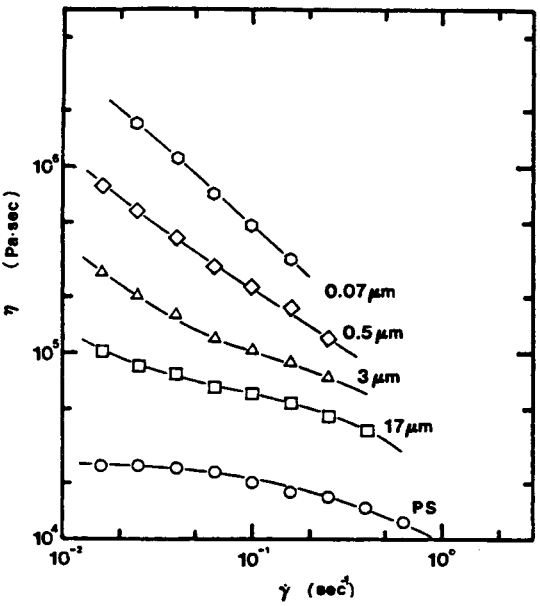

Fig. 5. Shear viscosity η of the PS and uncoated $CaCO_3$ compounds ($\phi = 0.3$) as a function of shear rate at 180°C.

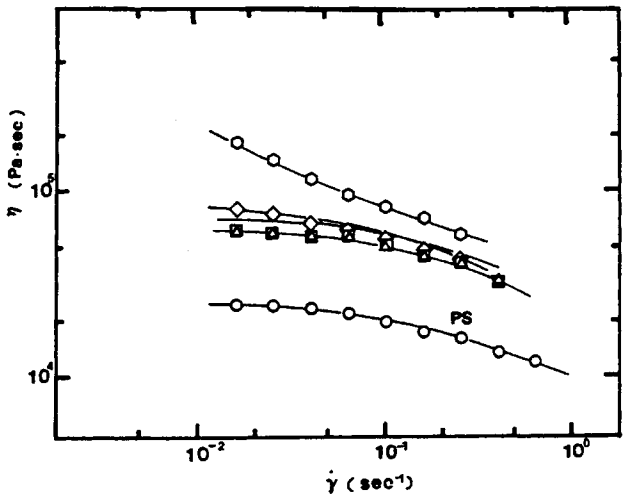

Fig. 6. Shear viscosity η of the PS and stearic-acid-coated $CaCO_3$ compounds ($\phi = 0.3$) as a function of shear rate: (○) 0.07 μm; (◇) 0.5 μm; (△) 3 μm; (□) 17 μm.

greater at the lowest shear rates for the compounds with the smallest particles.

The viscosity of the compounds of the stearic acid coated particles are in all cases smaller than those with the initial uncoated particles. We may define a viscosity reduction function:

$$H(\dot{\gamma}) = \frac{\eta(\dot{\gamma}, \phi, \text{uncoated}) - \eta(\dot{\gamma}, \phi, \text{coated})}{\eta(\dot{\gamma}, \phi, \text{uncoated})} \tag{7}$$

We tabulate values of $H(\dot{\gamma})$ in Table III. It may be seen that $H(\dot{\gamma})$ is positive in all cases. It increases in magnitude with decreasing particle size and decreasing shear rate. At a shear rate of 0.025 s^{-1}, the values of $H(\dot{\gamma})$ is 0.91 for the 0.07-μm particles and 0.25 for the 17-μm particles.

TABLE III
Viscosity Reduction by Stearic Acid Coating of $CaCO_3$ Particles ($\phi = 0.3$)

Particle diameter (μm)	$\dot{\gamma}(s^{-1})$	$H(\dot{\gamma})$
0.07	0.025	0.91
0.07	0.063	0.86
0.07	0.16	0.77
0.5	0.025	0.87
0.5	0.063	0.76
0.5	0.16	0.64
3	0.025	0.70
3	0.063	0.54
3	0.16	0.48
17	0.025	0.25
17	0.063	0.12
17	0.16	0.13

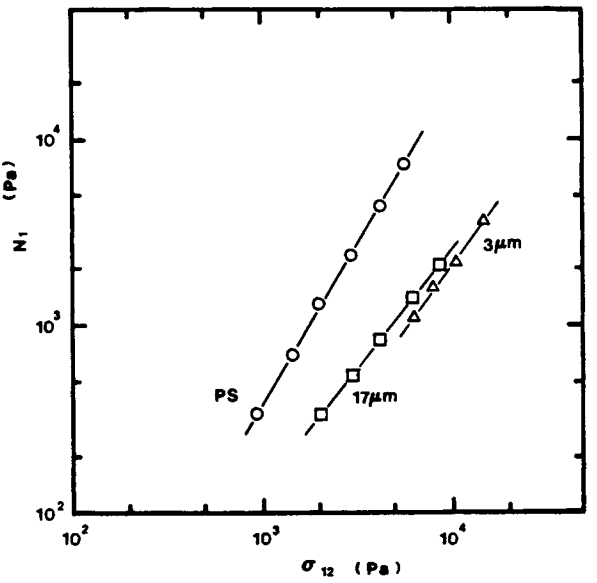

Fig. 7. Principal normal stress differences N_1 of the PS/$CaCO_3$ (uncoated) compounds as a function of shear stress σ_{12}; $\phi = 0.3$.

Principal Normal Stress Difference

In Figures 7 and 8, we plot the principal normal stress difference N_1 at a specified σ_{12} for the PS/$CaCO_3$ compounds. The compounds generally exhibit lower N_1 at a specified σ_{12} than the PS. The decrease is the greatest for the smallest particles.

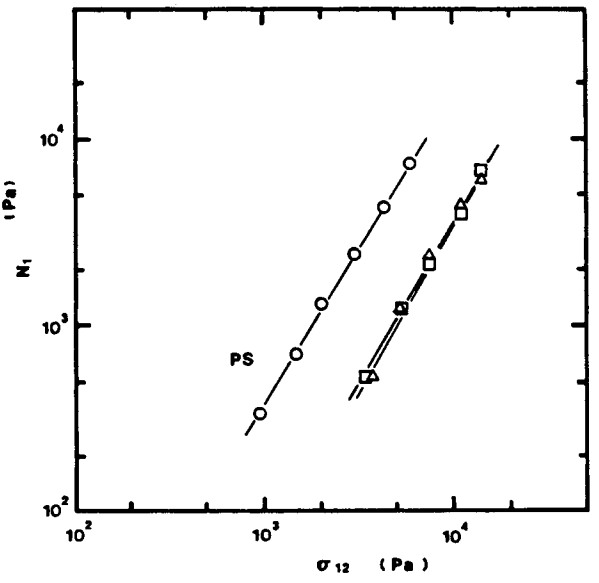

Fig. 8. Principal normal stress difference N_1 of the PS/$CaCO_3$ (stearic-acid-coated) compounds as a function of shear stress σ_{12}; $\phi = 0.3$: (□) 17 μm; (△) 3 μm.

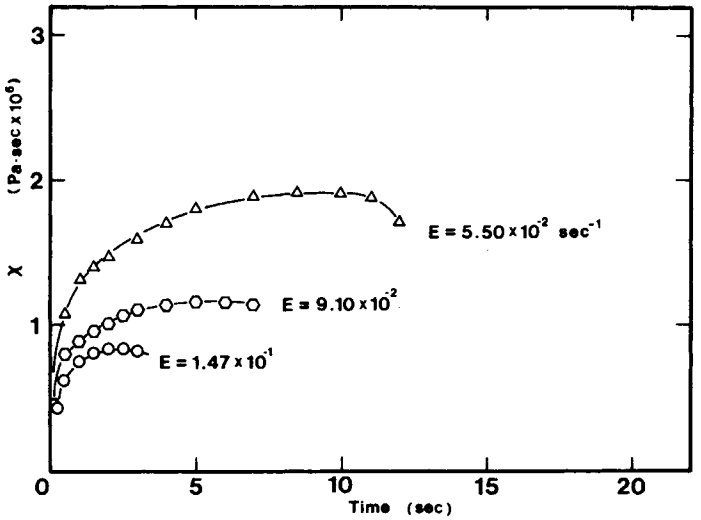

Fig. 9. Elongational viscosity as a function of time for different stretch rates for the PS/$CaCO_3$ compounds with d_p = 0.07 μm (uncoated particles); ϕ = 0.3.

Elongational Viscosity

The elongational viscosity of the PS melt was found to be essentially that found in earlier studies of this material in our laboratories.[20,22,23] A steady state elongational viscosity was achieved. This is equal to $3\eta_0$ at low stretch rates and increases at higher stretch rates.

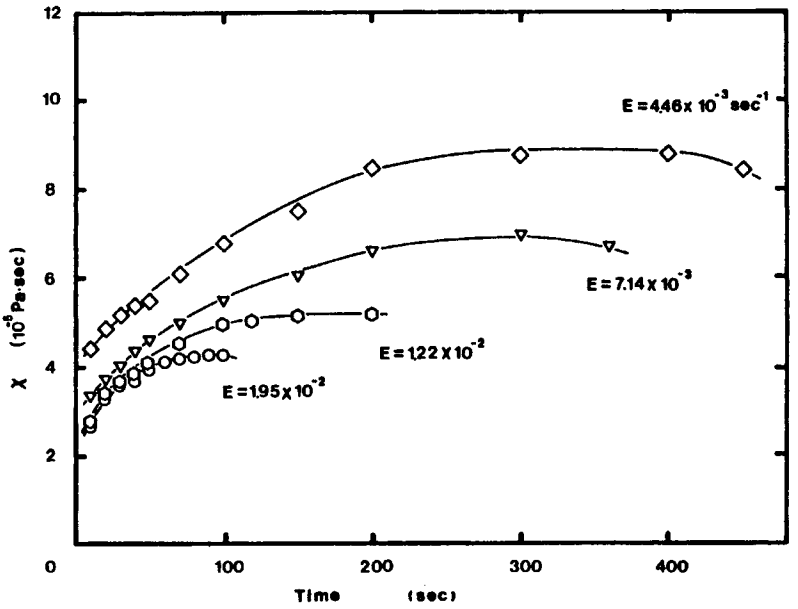

Fig. 10. Elongational viscosity as a function of time for different stretch rates for PS/$CaCO_3$ compounds with d_p = 0.07 μm (coated particles); ϕ = 0.3.

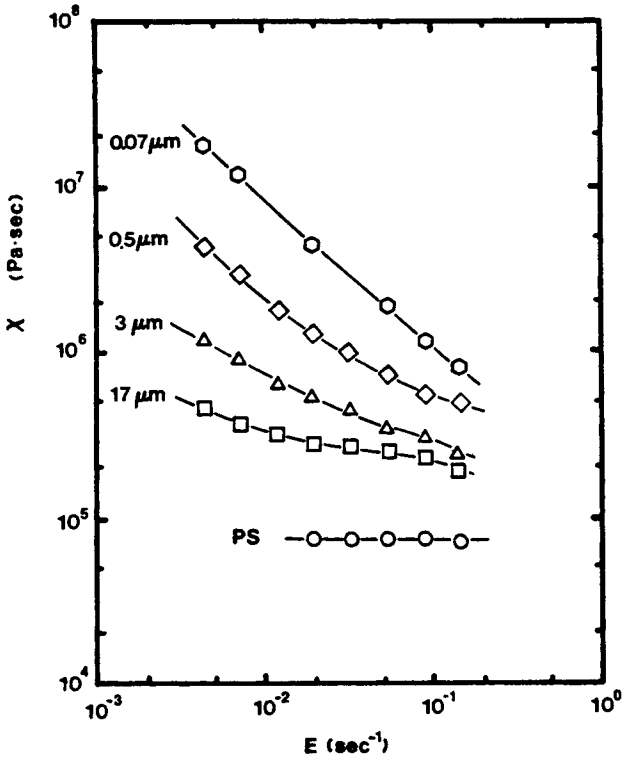

Fig. 11. Steady state elongational viscosity χ as a function of stretch rate for the uncoated PS/$CaCO_3$ compounds; $\phi = 0.3$.

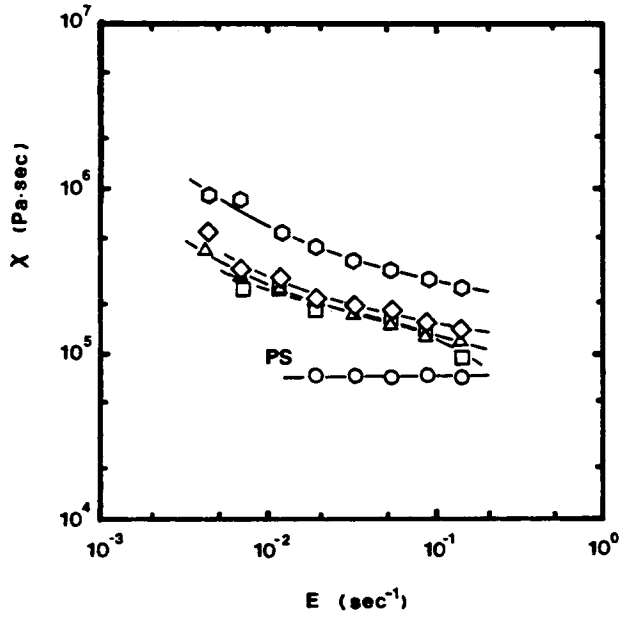

Fig. 12. Steady state elongational viscosity χ as a function of stretch rate for the stearic acid coated PS/$CaCO_3$ compounds; $\phi = 0.3$: (○) 0.07 μm; (◇) 0.5 μm; (△) 3 μm; (□) 17 μm.

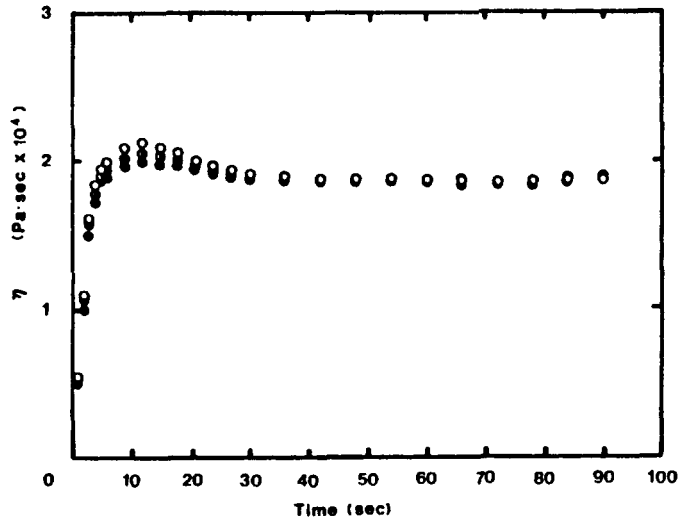

Fig. 13. Transient shear stress in a sequential two step deformation for PS-$\dot{\gamma} = 0.16\ s^{-1}$. Interval(s): (○)—; (●) 210; (◑) 510; (Φ) 1800.

In Figures 9 and 10, we show typical plots of elongational viscosity versus time for PS/$CaCO_3$ compounds at various stretch rates. Steady states are achieved for a wide range of conditions.

In Figures 11 and 12, we plot steady state elongational viscosities χ vs. stretch rate for the uncoated and coated PS/$CaCO_3$ compounds. It may be seen that the elongational viscosity increases with addition of particles. The extent of viscosity rise increases with decreasing particle size. It is greater for the uncoated particles than for those coated with stearic acid. The elongational viscosity

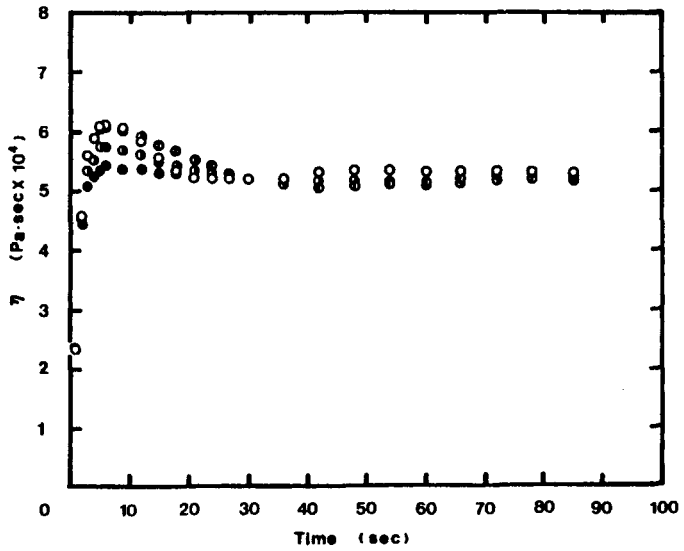

Fig. 14. Transient shear stress in a sequential two step deformation for PS/$CaCO_3$ compounds (uncoated): $\dot{\gamma} = 0.16\ s^{-1}$; $d_p = 17\ \mu m$; $\phi = 0.3$. Interval(s): (○)—; (●) 210; (◑) 510; Φ 1800.

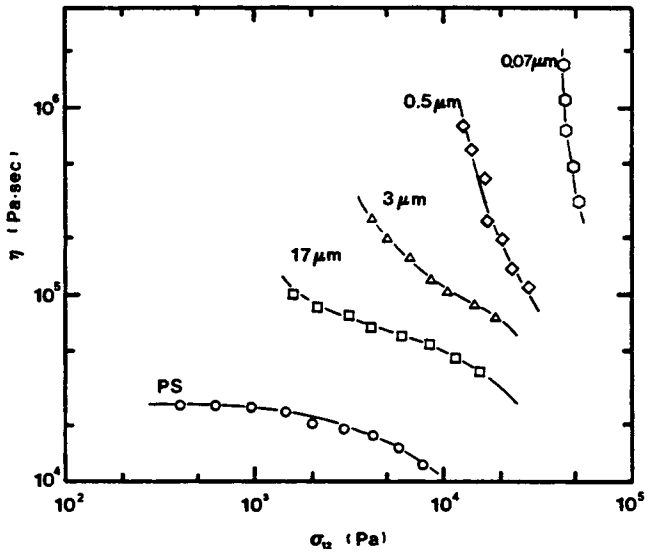

Fig. 15. Shear viscosity vs. shear stress for PS and PS/$CaCO_3$ (uncoated) systems; $\phi = 0.3$.

function χ is in general a decreasing function of stretch rate for the compounds and does not become constant at low rates of deformation.

Sequential Deformation Histories

Transient shear viscosities as a function of a time in a deformation history, where the melt is subjected to a steady shear flow for a period of 90 s followed by periods of rest of hundreds of seconds and a second constant shear rate history. Typical shear viscosity histories are shown in Figures 13 and 14. Generally the

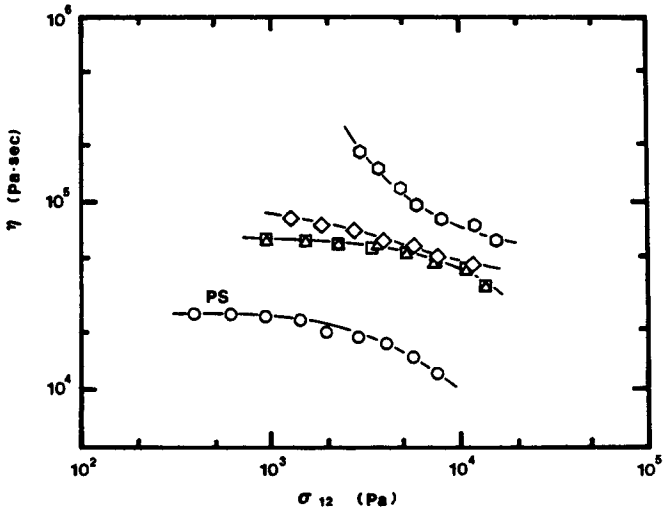

Fig. 16. Shear viscosity is shear stress for PS and PS/$CaCO_3$ (coated) systems; $\phi = 0.3$: (○) 0.07 μm; (◇) 0.5 μm; (△) 3 μm; (□) 17 μm.

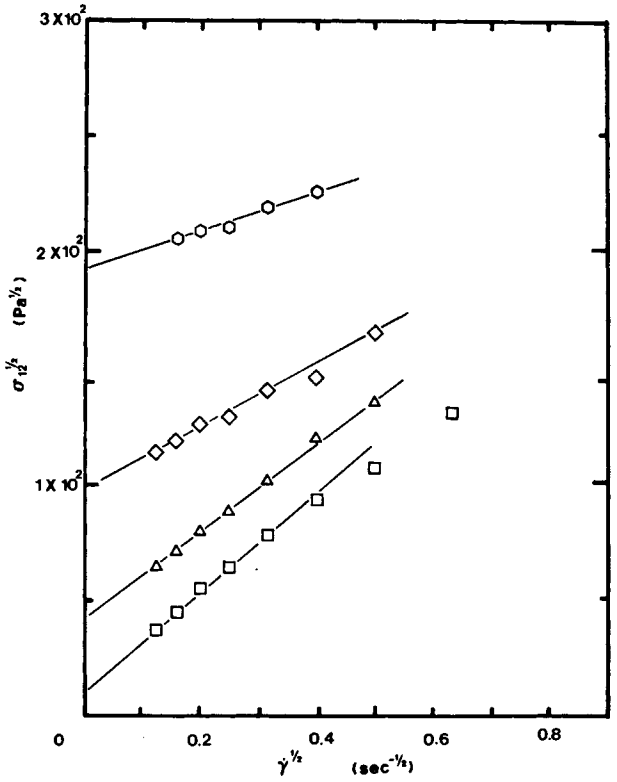

Fig. 17. Plot of $\sigma_{12}^{1/2}$ vs. $\dot{\gamma}^{1/2}$ (Casson plot) to determine yield values (ϕ = 0.3): (a) uncoated $CaCO_3$/PS, (b) coated $CaCO_3$/PS. (○) 0.07 μm; (◇) 0.5 μm; (△) 3 μm; (□) 17 μm.

viscosity overshoot behavior in the second flow period is substantially reduced. The longer the rest period the greater the reduction in shear viscosity. The effect is much larger in the particle filled melts.

INTERPRETATION

Shear Viscosity

The decreasing character of the viscosity shear rate function and the general increasingly negative slope at low shear rates suggests yield values. In Figures 15 and 16 we plot viscosities vs. shear stress. The tendency towards yield values is seen. This is most striking with the uncoated particles.

Following Kataoka et al.,[17,19] we have estimated yield values in our systems by fitting the empirical equation of Casson:

$$\sigma_{12}^{1/2} = Y_s^{1/2} + k_s \dot{\gamma}^{1/2} \tag{8}$$

to the data. A plot of $\sigma_{12}^{1/2}$ vs. $\dot{\gamma}^{1/2}$ is shown in Figure 17. The yield values so determined are tabulated in Table IV. Yield values were also estimated from the η–σ_{12} plots. We also summarize these in Table IV. The magnitude of the

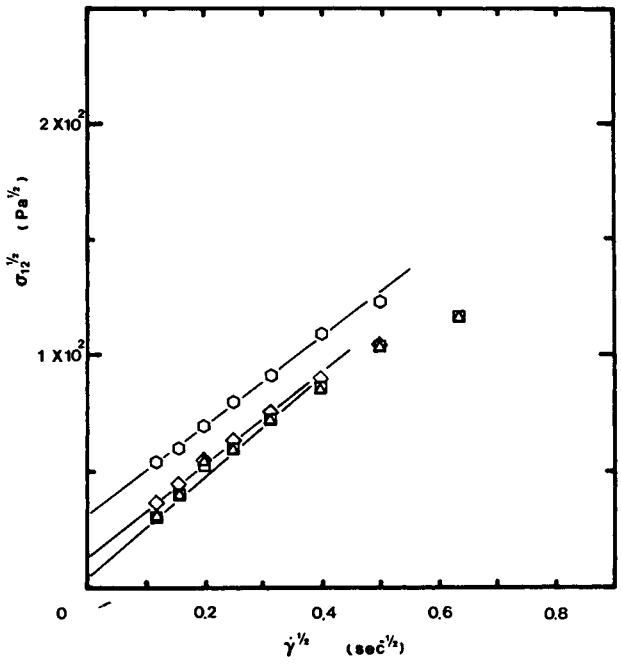

(b)

Fig. 17 (*Continued from the previous page.*)

yield values increase with decreasing particle size. Yield values have been noted by various earlier investigators.[4,6,9,14,17,19,21,23]

In Figure 18, we present a logarithmic plot of yield value Y vs. particle size including our own data and that of the literature on filled polymer melts. Y exhibits an approximately inverse first power dependence upon particle size. There is some scatter in the data.

Experimental studies of the shear viscosity of suspensions of similar small particles in Newtonian fluid matrices also show yield values which increase with decreasing particle size. Examination of experimental data on such suspensions show a similar inverse first power dependence upon particle size.[35]

TABLE IV
Estimated Yield Values for PS/$CaCO_3$ Systems

Investigator	Particle size (μm)	Coating	Y_s (Pa) Casson [eq. (8)]	Y_s (Pa) η–σ_{12} plot
This research	0.07	no	38×10^3	40×10^3
	0.07	yes	1.0×10^3	Unclear
	0.5	no	9.0×10^3	10×10^3
	0.5	yes	0.16×10^3	Unclear
	3	no	1.6×10^3	$\sim 1.5 \times 10^3$
	3	yes	$< 0.1 \times 10^3$	Unclear
	17	no	0.1×10^3	Unclear
	17	yes	$< 0.1 \times 10^3$	Unclear
Tanaka and White[21]	0.5	no	9.0×10^3	12×10^3
	0.5	yes	0.16×10^3	Unclear

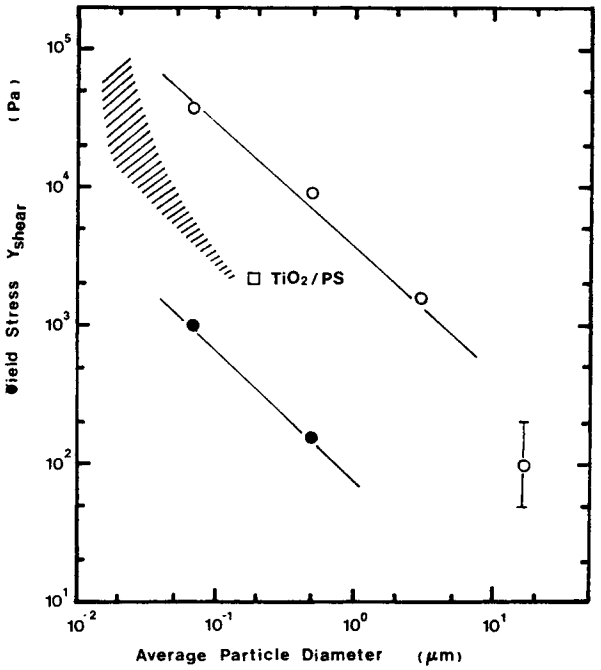

Fig. 18. Yield value as a function of particle size on a logarithmic plot (ϕ = 0.3): (○) uncoated $CaCO_3$/PS; (●) coated $CaCO_3$/PS; (⁄⁄) CB/PS.

It is also of interest to compare the results of our experiments with theories of concentrated suspensions. The concentrated suspension cell theory model of Tanaka and White[36] predicts an inverse first power dependence of the yield

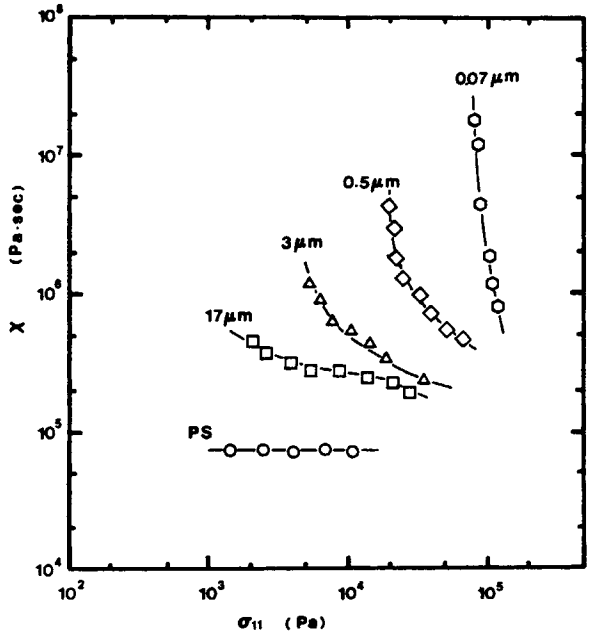

Fig. 19. Elongational viscosity as a function of tensile stress for PS and uncoated PS/$CaCO_3$; ϕ = 0.3.

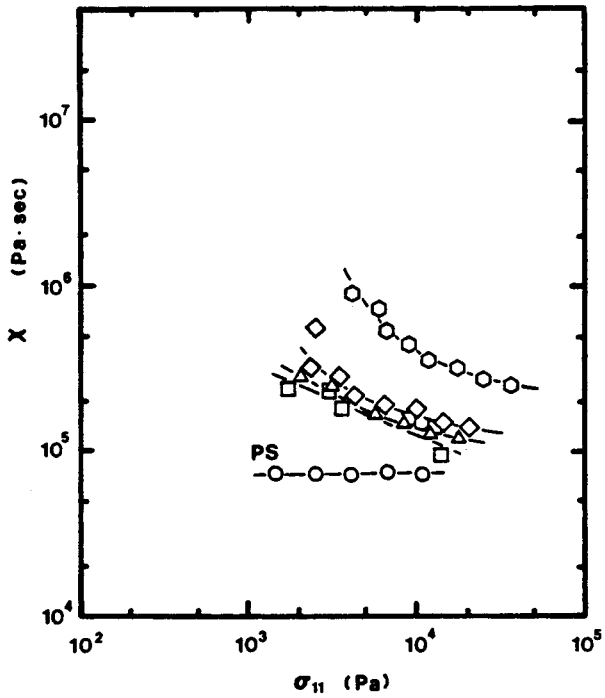

Fig. 20. Elongational viscosity as a function of tensile stress for PS and coated PS/$CaCO_3$; ϕ = 0.3. (○) 0.07 μm; (◇) 0.5 μm; (△) 3 μm; (□) 17 μm.

value for electrostatic forces and third power for inverse sixth power London forces. This cell model does not consider the aggregation of particles which is frequently associated with yield values in suspensions.[37–39] A theory of concentrated suspensions yield values based on flocculation behavior of Firth and Hunter[39,40] does predict an inverse particle diameter dependence.

Elongational Viscosity

In Figures 19 and 20, we plot the elongational viscosity χ as a function of tensile stress. Tendencies towards yield values Y_e are observed. These values are summarized in Table V. We have also determined yield values with Casson plots of the form

$$\sigma_{11}^{1/2} = Y_e^{1/2} + k_e E^{1/2} \tag{9}$$

Ratios of the yield value in extension Y_e to that in shear $Y_s(Y_e/Y_s)$ of order 1.4–1.9 are obtained. The values of Y_e for the coated particles are much smaller.

The ratios of Y_e/Y_s obtained are similar in magnitude to those reported by Tanaka and White.[21] They agree with the magnitudes predicted by the von Mises criterion for plastic flow of solids[36]

$$\text{tr } \mathbf{P}^2 = 2Y_s^2 \tag{10}$$

where $\mathbf{P}$ is the deviatoric stress tensor. This has been used as the basis of a theory of plastic–viscoelastic fluids which has been applied to the flow of particle filled polymer melts.[42,43] We will investigate this in more detail in later papers.

TABLE V
Yield Values for Elongational Flow for PS/$CaCO_3$ Systems

Investigator	Particle size (μm)	Coating	Y_e (Pa)	Y_e/Y_s
This research	0.07	no	10×10^3	1.84
	0.07	yes	1.6×10^3	1.60
	0.5	no	8.5×10^3	0.94
	0.5	yes	0.26×10^3	1.63
	3	no	2.3×10^3	1.44
	3	yes	—	—
	17	no	1.9×10^3	1.90
	17	yes	—	—
Tanaka and White[21]	0.5	no	1.6×10^4	1.78
	0.5	yes	—	—

Surface Coating

Viscosities and yield values are substantially lowered by coating the surface of the $CaCO_3$ particles with stearic acid. The surface coating would clearly seem to decrease particle–particle interaction. As we have noted, yield values in suspensions have long been associated with interparticle flocculation.[37–39] Presumably in coating $CaCO_3$ with stearic acid, the COOH groups tie to the surface and the hydrocarbon chains point away from the interface into the bulk phase. Interparticle interaction should be reduced. The coated $CaCO_3$ particles would be expected to behave more like nonpolar particles such as carbon black. Such a tendency may be seen in Figure 18.

Principal Normal Stress Differences

In agreement with earlier investigators[14,20,21,23] it is found that normal stresses at fixed shear stress are reduced. However as particle size decreases it becomes increasingly difficult to measure normal stresses as indicated earlier.

The normal stress transients of Figure 2 require added emphasis. Generally the materials are squeezed into place in the gap between the cone and the plate, which creates finite sizeable normal forces. When the materials involved exhibit yield stresses the squeezing force decays to a finite value. This finite value seems to increase with the magnitude of the yield stress. The normal force measurements from the subsequent shear flow are difficult to interpret. Certainly one must be wary of the short time transients in all cases. If the finite value to which the squeezing force decays is of the same order or greater than the shear flow normal force the problem becomes increasingly difficult. Here the baseline becomes uncertain. In a separate study we are analyzing this behavior in terms of our plastic viscoelastic fluid theory.[44]

This research was supported in part by the National Science Foundation under NSF Grant CPE-8001744. We would like to thank Pfizer for supplying the series of well-characterized $CaCO_3$ particles with and without stearic acid coating and Dow Chemical for the polystyrene.

References

1. L. Mullins, *J. Phys. Coll. Chem.*, **54**, 539 (1950).
2. M. L. Studebaker, Proceedings of the Third Rubber Technology Conference, 1954, p. 623.
3. C. C. McCabe and N. Mueller, *Trans. Soc. Rheol.*, **5**, 329 (1961).

4. N. V. Zakharenko, F. S. Tolstokhina, and G. M. Bartenev, *Rubber Chem. Technol.*, **35I,** 326 (1962).
5. J. R. Hopper, *Rubber Chem. Technol.*, **40I,** 463 (1967).
6. F. M. Chapman and T. S. Lee, *Soc. Plast. Eng. J.*, **26**(1), 37 (1970).
7. P. P. A. Smit and A. K. van der Vegt, *Kautschuk Gummi*, **23,** 147 (1970).
8. E. A. Collins and J. T. Oetzel, *Rubber Age* (March), (1970).
9. G. V. Vinogradov, A. Ya Malkin, E. P. Plotnikova, O. Y. Sabsai, and N. E. Nikolayeva, *Int. J. Polym. Mater.*, **2,** 1 (1972).
10. F. Nazem and C. T. Hill, *Trans. Soc. Rheol.*, **18,** 87 (1974).
11. C. D. Han, *J. Appl. Polym. Sci.*, **18,** 821 (1974).
12. J. L. White and J. W. Crowder, *J. Appl. Polym. Sci.*, **18,** 1013 (1974).
13. N. Nakajima and E. A. Collins, *Rubber Chem. Technol.*, **48,** 615 (1975).
14. N. Minagawa and J. L. White, *J. Appl. Polym. Sci.*, **20,** 501 (1976).
15. M. S. Boaira and C. E. Chaffey, *Polym. Eng. Sci.*, **17,** 715 (1977).
16. Y. Chan, J. L. White, and Y. Oyanagi, *Trans. Soc. Rheol.*, **22,** 507 (1978).
17. T. Kataoka, T. Kitano, M. Sasahara, and K. Nishijima, *Rheol. Acta* **17,** 149 (1978).
18. C. D. Han, C. Sanford, and H. J. Yoo, *Polym. Eng. Sci.*, **18,** 849 (1978).
19. T. Kataoka, T. Kitano, Y. Oyanagi, and M. Sasahara, *Rheol. Acta*, **18I,** 635 (1979).
20. V. M. Lobe and J. L. White, *Polym. Eng. Sci.*, **19,** 617 (1979).
21. H. Tanaka and J. L. White, *Polym. Eng. Sci.*, **20,** 949 (1980).
22. L. Czarnecki and J. L. White, *J. Appl. Polym. Sci.*, **25,** 1217 (1980).
23. J. L. White, L. Czarnecki, and H. Tanaka, *Rubber Chem. Technol.*, **53,** 823 (1980).
24. C. D. Han, T. van der Weghe, P. Shete, and J. R. Haw, *Polym. Eng. Sci.*, **21,** 196 (1981).
25. S. Toki and J. L. White, *J. Appl. Polym. Sci.*, **27,** 3171 (1982).
26. S. Middleman, *The Flow of High Polymers*, Wiley, New York, 1967.
27. K. Walters, *Rheometry*, Halstead, London, 1975.
28. R. G. King, *Rheol. Acta*, **5,** 35 (1966).
29. B. L. Lee and J. L. White, *Trans. Soc. Rheol.*, **18,** 467 (1974).
30. J. F. Hutton, *Rheol. Acta*, **14,** 979 (1975).
31. D. M. Binding, J. F. Hutton, and K. Walters, *Rheol. Acta*, **15,** 540 (1976).
32. S. Suto, J. L. White, and J. F. Fellers, *Rheol. Acta*, **21,** 62 (1982).
33. Y. Ide and J. L. White, *J. Appl. Polym. Sci.*, **22,** 2061 (1978).
34. J. Meissner, Rheol. Acta, **8,** 78 (1969).
35. B. A. Firth, J. Colloid Interf. Sci., *57*, 257 (1976).
36. H. Tanaka and J. L. White, J. Non-Newt. Fluid Mech., *7*, 333 (1980).
37. E. L. McMillen, J. Rheology, *3*, 179 (1932).
38. H. Freundlich and A. D. Jones, J. Phys. Chem., *40*, 1217 (1936).
39. B. A. Firth and R. J. Hunter, *J. Colloid Interface Sci.*, **57,** 248 (1976).
40. B. A. Firth and R. J. Hunter, *J. Colloid Interface Sci.*, **57,** 266 (1976).
41. W. Prager and P. Hodge, *Theory of Perfectly Plastic Solids*, Wiley, New York, 1951.
42. J. L. White, *J. Non-Newt. Fluid Mech.*, **5,** 177 (1979).
43. J. L. White and H. Tanaka, *J. Non-Newt. Fluid Mech.*, **8,** 1 (1981).
44. Y. Suetsugu and J. L. White, to appear.

Received June 8, 1982
Accepted November 29, 1982